

# Soil water retention curves of a silty clayey sand compacted at different dry density

Roberta Ventini<sup>1\*</sup>, Marianna Pirone<sup>2</sup>, and Claudio Mancuso<sup>2</sup>

<sup>1</sup>Ministry of Infrastructures and Transport, Interregional Public Works Department, 50122 Firenze, Italy

<sup>2</sup>University of Napoli Federico II, Department of Civil, Building and Environmental Engineering, 80125 Napoli, Italy

**Abstract.** The study of the hydraulic behaviour of compacted soils in partially saturated conditions is essential for understanding the engineering performance of geotechnical structures such as river embankments. The paper presents the results of an experimental study focusing on the effects of the initial water content and dry density on soil water retention curve (SWRC) and volume change of a compacted soil mixture under hydraulic loading. For this purpose, soil specimens compacted at different water contents (dry, wet and optimum water content), chosen on the basis of standard Proctor compaction test, were used. Specimens of a mixture composed of 70% Ticino sand (TS) and 30% Pontida silt (PON) have been tested. This is a heterogeneous mixture of sand and silt, that usually constitute the embankments of tributaries of river Po (Italy). The SWRCs along drying paths were performed by means of evaporation tests starting from the saturated conditions gained in permeameter tests. For the investigation of the change in the void index during the evaporation test, the volume variation of the tested specimens was estimated by means of a calliper and photographic comparison. Changes in the SWRCs are consistent with changes in specimen initial condition while the soil volume change exhibited at the end of evaporation test is always negligible.

## 1 Introduction

The type of soil and the compaction technique used in the construction of embankments and dams play a fundamental role in determining the type and rate at which any adverse phenomena may occur. The soil texture is in fact significantly influenced by the compaction process, with important implications on hydraulic properties (e.g. [1]) and shear strength (e.g. [2]).

Many studies (e.g. [3]) have shown that the microstructure of a compacted soil strongly depends on the preparation method used. Typical examples are the variation in the hydraulic conductivity of clay soils when compacted at different water contents and the change in shear strength parameters as function of the compaction technique used.

As it is widely recognized, compaction significantly influences soil hydraulic properties, soil water retention and soil water flow [1]. The effects of water content and method of compaction on the permeability of compacted silty clay were determined by [4]. It emerged the difficulties in the selection of an appropriate value of the permeability for use in problems involving seepage or pore pressure dissipation due to the great variability in permeability with compaction conditions. Experimental results discussed in [5] indicate that initial water content, selected from the standard AASHTO test, has considerable influence on the resulting structure (and aggregation), which in turn influences the soil–water characteristics. Also, [6] showed that the pore and

aggregate structure and, therefore, the soil–water retention curve (SWRC) of clay are influenced by the compaction conditions. Typically, compacted specimens may have a distinct microstructure and therefore, if prepared in several ways, behave differently in response to external changes such as hydrological ones.

Therefore, experimental determination of the effects of compaction on the hydromechanical behaviour of soils is essential for a reliable assessment of the stability of earthworks, to provide guidance in defining compaction specifications and, finally, as an aid in predicting the probability and type of collapse that may affect such structures. A methodological approach for the investigation of the hydromechanical response of river embankment, based on laboratory testing and numerical modelling was proposed by [7]. The Authors [7] proved the key role played by the characterization of a compacted mixture of sand and finer material under partially saturated conditions to analyse properly the performance of a typical embankment of the main river Po tributaries (Italy) under transient seepage.

In this paper, the main factors influencing soil–water retention curves of compacted fine-grained soils are investigated; evaporation tests and volume change estimation determined on mixtures compacted at different dry density are presented and discussed. In particular, the influence of different compaction water contents and initial dry densities on the soil–water retention curve is described in depth along with the volume change measured during evaporation tests.

\* Corresponding author: [roberta.ventini@unina.it](mailto:roberta.ventini@unina.it)

## 2 Materials and methods

Embankments built along the tributaries of the Po River (Italy) are generally composed of a heterogeneous mixture of sand, silt and sometimes clay, and frequently founded on clayey and silty deposits. To experimentally characterize a material for a river embankment to be reproduced in geotechnical centrifuge tests [8, 9] within the PRIN 2017 project called "Risk Assessment of Earth Dams and River Embankment to Earthquakes and Floods (REDREEF)", a mixture consisting of 70% Ticino Sand (TS) and 30% Pontida clayey sandy silt (PON) was selected (TS70%-PON30%). Here, the soil water retention curves determined on three mixtures TS70%-PON30%, compacted at different water contents and initial dry densities are carried out.

Ticino Sand [10] and Pontida clayey sandy silt [7] are well-known Italian soils subjected to intensive previous experimental campaigns. The particle size distributions of the individual components (TS and PON) and the mixture are shown in Fig. 1. The mixture prepared in the laboratory is a silty clayey sand with a low plasticity. In addition, the physical properties are reported in Table 1.

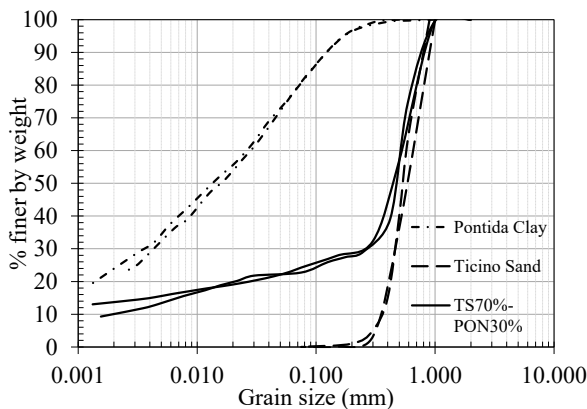


Fig. 1. Grain size distributions (after [7]).

**Table 1.** Average on index properties of the tested materials ( $e_{min}$  minimum value of void ratio,  $e_{max}$  maximum value of void ratio,  $G_s$  specific soil density,  $D_{50}$  mean particle size,  $U_c$  uniformity coefficient, LL limit liquid, PL plastic limit, PI plasticity index).

Soil	$e_{min}$	$e_{max}$	$G_s$	$D_{50}$ mm	$U_c$	LL %	PL %	PI %
TS <sup>1</sup>	0.574	0.923	2.671	0.574	1.83	-	-	-
PON <sup>1</sup>	-	-	2.744	0.015	-	23.61	13.13	10.48
TS70%- PON30% <sup>1</sup>	0.236	0.953	2.684	0.458	246.06	17.66	10.23	7.42

<sup>1</sup> From [7]

Soils used for the construction of embankment and dams are commonly compacted to obtain better performance of earthen structures. As it is well known, compaction provides an artificially increase of the dry density of the soil through the application of mechanical energy, thereby reducing its compressibility, increasing its (peak) shear strength as well as reducing undesirable effects produced by frost and imbibition or drying phenomena. The compaction conditions adopted in situ

can be simulated in the laboratory through the dry density ( $\gamma_d$ ) - water content ( $w$ ) curve by using a standard procedure. In this regard, the Proctor test is a dynamic test that consists of applying a known compaction energy to the soil placed in a mould of standard dimensions by means of a piston dropped from an assigned standard height. The Standard Proctor (SP) test [11] represents a compaction procedure typically used as a reference for earthworks so it has been chosen for the mixture studied here. The compaction curve is shown in Fig. 2. To investigate the effect of the initial  $\gamma_d$ - $w$  condition on the hydraulic response of the tested mixture, compacted by applying SP energy, three samples were reconstituted and compacted at the dry, optimum and wet conditions, the symbols shown in Fig. 2.

In addition, particle size analyses performed after Proctor compaction showed no significant grain breakage.

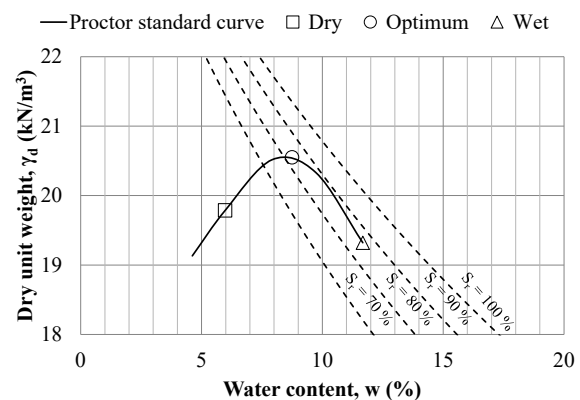


Fig. 2. Compaction curve of the TS70%-PON30% mixture.

### 2.1 Test procedure

The permeability and water retention characteristics are strongly influenced by the soil texture resulting from compaction [12]. As it is well known, the determination of hydraulic properties is time-consuming. One of the available procedures for determining the saturated hydraulic conductivity ( $k_{sat}$ ) is to perform a permeameter test at constant load. For this purpose, immediately after compaction, the compacted specimens were taken from the Proctor mould using a cylindrical metal ring with diameter  $d = 7.21$  cm and height  $h = 6.08$  cm which includes two holes to house the tensiometers installed 3 cm apart (respectively 1.50 and 4.50 cm from the top). In the permeameter, used for  $k_{sat}$  measurement, the holes are closed to allow the flow of pressurised water until saturation. The gradient of pore water pressure between the base and the top of the specimen was imposed equal to 5 kPa. The saturation process in the permeameter was assumed to be complete when a steady-state condition characterized by equal water flow rates in and out was reached [13]. The saturated hydraulic conductivity was then determined using Darcy's law. The  $k_{sat}$  values measured for each specimen are shown in Table 2, where different values, in terms of several orders of magnitude, are recorded with varying compaction condition. As reported in [14] and [15] on the dry side

of compaction optimum the coefficient of permeability tends to be relatively higher than that of specimens compacted at wet of optimum water content because the increasing water content results in reorientation of clay particles and reduction in the size of interparticle pores [16]. However, it is noteworthy to highlight the considerable variability, of four orders of magnitude of the coefficient of permeability,  $1.10E-05$  m/s and  $8.59E-09$  on the dry and wet side respectively, obtained on the same soil at the scale of the laboratory specimen, by varying only the compaction initial condition.

The porosity  $n$  measured after the specimen preparation ( $n_{in}$ ) and after the test in the permeameter ( $n_p$ ) are also reported in Table 2. The different values are probably due to a volumetric collapse undergone by all specimens during saturation, which leads to a rearrangement of the soil structure to a state of higher density. The wet specimen characterized by an initial higher water content and a lower dry density than the other two specimens underwent a greater volumetric collapse. As reported by [17], the volumetric collapse occurs mainly in dry and loose soils. So, in the specific case, the effect of the initial dry density during wetting is predominant according to [18]. The fact that the dry density after compaction is the predominant parameter affecting wetting-induced deformations under vertical stress is also confirmed by [17] and [19].

**Table 2.** Properties of the tested specimens.

Specimen	Compaction	$\gamma_d$ kN/m <sup>3</sup>	w %	$n_{in}$ -	$n_p$ -	$k_{sat}$ m/s
PSD7	Dry	19.19	5.53	0.269	0.230	1.10E-05
PSO13	Optimum	19.90	8.79	0.245	0.214	2.19E-08
PSW7	Wet	18.65	12.04	0.308	0.219	8.59E-09

After saturation, the soil water retention curve (SWRC) of the mixture along the main drying branch was determined by using in series a ku-pF (Umwelt-Geräte-Technik GmbH) commercial apparatus and a Richards plate described in [7, 13, 20-22]. In the ku-pF apparatus the saturated specimen is subjected to a drying process during which the water content (by weight) and suction up to 80 kPa (by small tip tensiometers) are measured and recorded. Subsequently, the same specimen is next placed in the Richards plate to collect data on the SWRC in the range of suction from 80 kPa to 1 MPa.

### 3 Experimental results

#### 3.1 Soil water retention curves

The experimental points determined for the three mixtures along with the best-fitting curves modelled by the Van Genuchten (VG) equation [23] are plotted in soil water retention plane in Fig. 3. In addition, the parameters of the VG model are reported in Table 3. It can be seen that as the matric suction increases, the volumetric water content of all specimens decreases at

different rates so the primary drying of the samples depends strongly on the compaction condition (Fig. 3). From Fig. 3, with increasing compaction water content, the air entry value (i.e., the point where the soil gives up water with increasing soil suction) increases. Also, in the suction range between 10 and 100 kPa, the soil-water retention curve is dependent on the initial conditions. However, for high suction and smaller water contents, the SRWCs of dry and optimum specimens tend to converge towards similar values of the residual volumetric water content so as stated by [15]. Fig. 3 and Table 3 showed that both  $\alpha$ , a parameter related to AEV and inversely proportional to mean pore diameter, and  $\theta_{sat}$ , a parameter related with the porosity, decrease as the compaction water content increases. The correlation of parameters related to grain size and grain distribution to compaction water content seems to reinforce the assumption, widely reported in literature [5, 15], that the initial water content has a much larger influence on the water retention curve than the initial dry density.

The specimen compacted at the dry side of the optimum has the steepest SWRC in the transition zone as also reported by [24] for a Lanzhou silt compacted at the standard compaction energy and different water content.

Therefore, although the same compaction technique was used in the laboratory, the different initial  $\gamma_{d-w}$  condition appears to have a significant effect on the hydraulic response of the soil in terms of both SWRC and the saturated hydraulic conductivity (Table 2). To understand the influence of compaction water content on hydraulic response, several investigations were made by using microscopic images by several Authors (e.g. [24-25]). It emerged that the soil compacted at the dry of optimum water content has a flocculated structure with aggregate of clay sticks to the silt grains [25] while the soil compacted at the wet of optimum water content has a dispersed structure represented by clay particles paste on the silt grain and the optimum specimen has an intermediate structure. Increasing water content generally results in an increased ability to break down clay aggregates and to eliminate inter-aggregate pores by making the mixture more impervious with the SWRC typical of the finer soils [4]. So, the soil microstructure depends on the initial  $\gamma_{d-w}$  condition and it follows a significative variety in the hydraulic soil behaviour.

**Table 3.** Van Genuchten model parameters for the tested specimens.

Specimen	Compaction	$\theta_{sat}$ -	$\theta_r$ -	$n$ -	$\alpha$ 1/kPa
PSD7	Dry	0.240	0.1013	1.471	0.603
PSO13	Optimum	0.204	0.0005	1.134	0.093
PSW7	Wet	0.196	0.0100	1.245	0.065

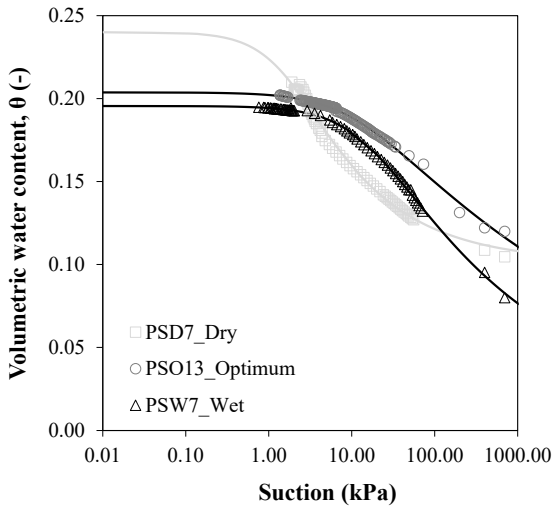


**Fig. 3.** Soil water retention curves of the TS70%-PON30% mixture tested specimens.

The results obtained at dry, wet and optimum were supported by other tests performed for the same  $\gamma_d$ - $w$  condition (Fig.4). In particular, the SWRCs obtained for the optimum specimens define a very narrow range of variation (Fig. 4b).

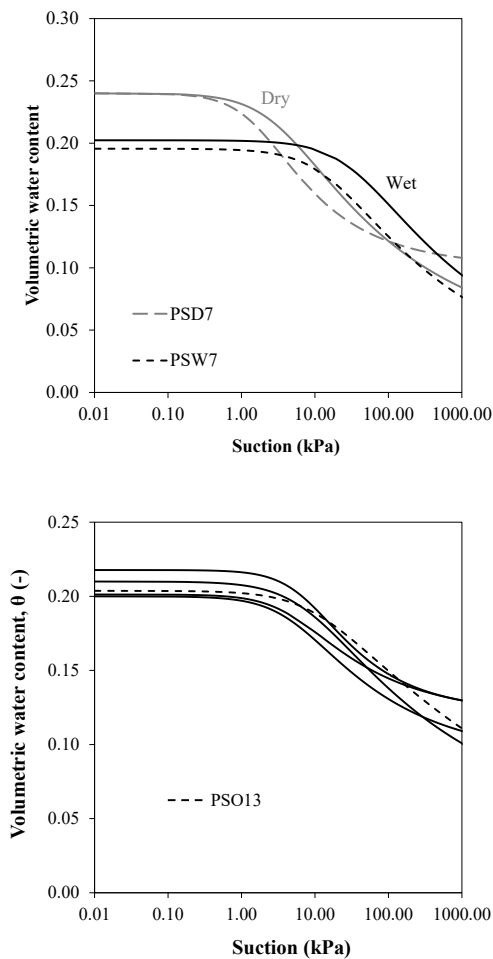


**Fig. 4.** Soil water retention curves for a) dry and wet and b) optimum mixture specimens.

The results of the entire experimental campaign, (number of soil specimen, N) N=5 at optimum, N=2 at wet side, N=2 at the dry side, are shown in Fig. 5. It is set up a trellis plot that allows to observe if any relationships between the soil porosity measured after saturation  $n_p$ , the saturated hydraulic conductivity  $k_{sat}$ , the dry density  $\gamma_d$ , the saturated volumetric water content  $\theta_{sat}$  and the air entry value  $AEV$ , establish.

A correlation between the soil porosity measured after saturation  $n_p$ ,  $\gamma_d$ , and  $\theta_{sat}$  can be identified. In particular,  $n_p$ , decreases as the dry density increase as expected (Fig. 5h). Then,  $\theta_{sat}$  results very close to  $n_p$ , pointing out that the soil specimen starts from fully saturation (Fig. 5i).

In addition, if the initial water content increases, the  $k_{sat}$  and the  $\theta_{sat}$  decrease and the relationship  $k_{sat} - \theta_{sat}$  (Fig. 5e) appears to be very similar to that reported by [26]. Therefore, the saturated permeability decreases as the AEV increases by following a power law (Fig. 5f) and AEV increases by passing from the dry to the wet water content, as shown in the  $\gamma_d$ - $AEV$  plane (Fig. 5c). The AEV increases as the  $\theta_{sat}$  decreases according to the increment of the suction at the air entry increases with decreasing initial porosity (Fig. 5a, j).

In the other graphs, a chaotic distribution of the experimental points can be observed, indicating the lack of a unique relationship between the variables correlated.

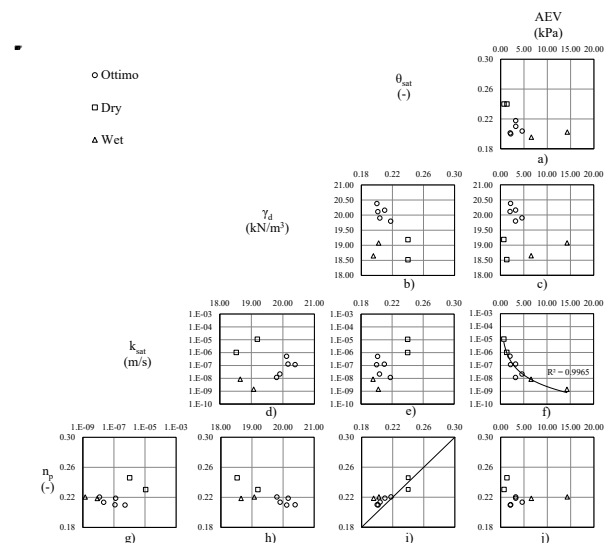


**Fig. 5.** Trellis plot: soil porosity  $n_p$ , saturated hydraulic conductivity  $k_{sat}$ , dry density  $\gamma_d$ , saturated volumetric water content  $\theta_{sat}$ , air entry value  $AEV$  plotted against each other.

### 3.2 Volume change estimation

In the literature several investigations on the influence of compaction conditions on the SWRC can be found but not all of them consider the volume change of the specimens. However, as reported by [27], the traditional method of interpretation the SWRC by neglecting any volume reduction clearly underpredicts the volumetric water content in the soil specimen.

The volume change during the evaporation test was estimated for all the specimens with two instruments: an analogic calliper with a resolution of 0.002 mm and a photo comparison. The former was fixed to the ku-pF apparatus, allowing for the measurement of the vertical settlements of the top of the specimen during the evaporation test. The measured axial strain at the end of evaporation test is equal to 1.13, 0.3 and 1.4% respectively for the dry, optimum and wet specimens. It decreases as the dry density increases in agreement with the established evidence that more compacted soils deform less than loose ones, and it also appears that the initial water content does not seem to influence univocally the volumetric response of the soil along a drying path. However, the axial strain of the wet specimen is the highest and it also true that if the soil is too wet it may crack due to desiccation shrinkage [14]. Therefore, also based on the change in porosity observed after saturation, it seems reasonable to assume that dry density has a more pronounced effect on both wetting-induced collapse and volume change under drying.

In order to estimate any compressive radial strains, a comparison was made between the photos of the two bases of the specimen at the beginning and at the end of the evaporation test. It was assumed, in a conservative way, that the radial deformation of the two bases is homogeneous along the height of the specimen. By overlapping the photos (Fig. 5) in a digital environment, it was found that variations in radial strain can be considered negligible (< 1%).



**Fig. 5.** Photo comparison before and after the evaporation test on the a) dry, b) optimum and c) wet compacted specimens.

It can therefore be stated that under the reproduced test conditions and with the type of soil tested, the changes in void index estimated during an evaporation test are of such a magnitude that it does not affect the

SWRCs determined. In fact, void index for wet specimen that exhibited the highest volume variation (i.e. 1.40%), changes from 0.271 to 0.262.

## 4 Concluding remarks

An experimental procedure to study the influence of different initial water contents and initial dry densities on the soil–water retention curves and saturated hydraulic conductivity of compacted soils was presented and discussed in the paper. Additionally, calliper measurements and photo comparisons were performed during evaporation tests to investigate the volume change of the specimens. For this purpose, compacted specimens at dry side, optimum and wet side of the Proctor standard curve of a silty clayey sand were prepared and tested.

It emerged that at the same compaction effort, the minimum saturated hydraulic conductivity is obtained at wet of optimum water content due to the different microstructure.

The SWRCs in terms of volumetric water content are dependent of the initial dry density and water content. However, in the high suction range at smaller water contents SWRC is independent of the initial conditions. It was observed that the porosity and so the saturated volumetric water content decreases with increasing dry density.

Furthermore, by estimating the volume change, it emerged that: a) both wetting-induced collapse and volume change under drying of the compacted specimens assume higher values for wet specimens and b) the volume change upon drying of the compacted soils is less than about 1.4%, so it can be assumed that the SWRCs of the tested soils are not affected, at least within the range of matric suction investigated in the ku- pF apparatus.

The results presented and discussed in the paper provide an insight into the hydraulic behaviour of the compacted specimens prepared with the same effort but at different points of the compaction curve. The effect of the initial compaction conditions on the soil water retention behaviour seems to be caused by the different microstructure determined by the dry density-water content coupling.

**Acknowledgments** This research was funded under the scheme for “Research Projects of National Relevance” (in Italian: Progetti di Ricerca di Rilevante Interesse Nazionale - PRIN), Bando 2017, grant number 2017YPMBWJ, promoted by the Italian Ministry of Education, University and Research (in Italian: Ministero dell’Istruzione, dell’Università e della Ricerca-MIUR).

## References

1. A. Klute. Tillage effects on the hydraulic properties of soils: A review. In: D.M. Krai and S. Hawkins (Editors), Predicting Tillage Effects on Soil Physical Properties and Processes. Am. Soc. Agron., Madison, WI, U.S.A., Spec. Publ. **44**, 29-41 (1982)

2. S. Ahmed, C.W. Lovell, S. Diamond. *J Geot Eng Div* **100**, 07-425 (1974)
3. F. Vinale, A. d'Onofrio, C. Mancuso, F. Santucci De Magistris, F. Tatsuoka. Opening Lecture at The Int. Conf. on Pre-Failure Deformation Characteristics of Geomaterials. Torino, Italy, **2**, 955-1007 (2001)
4. J.K. Mitchell, D.R. Hooper, J.K. Campanella. *J Soil Mec Found Div* **4**, 41-65 (1965)
5. S.K. Vanapalli, D.G. Fredlund, D.E. Pufahl. *Géotechnique* **49**, 143-159 (1999)
6. E. Romero, A. Gens, A. Lloret. *Eng Geol* **54**, 117-127 (1999)
7. R. Ventini, E. Dodaro, C.G. Gragnano, D. Giretti, M. Pirone. *Geosciences* **11**, 192 (2021)
8. R. Ventini, E. Dodaro, D. Giretti, M. Pirone, F. Zarattini, C.G. Gragnano, V. Fioravante, F. Gabrieli, G. Gottardi, C. Mancuso, *Analysis of transient seepage through a river embankment by means of centrifuge modelling*, in Proceedings of the 8th International Conference on Unsaturated Soils "Towards Unsaturated Soils Engineering", UNSAT, 2-5 May 2023, Milos, Greece (2023)
9. V. Girardi, E. Dodaro, R. Ventini, M. Pirone, C. G. Gragnano, D. Giretti, F. Zarattini, F. Gabrieli, *Numerical study of uplift induced levee failure for the design of a centrifuge test*, in Proceedings of Fifth International Conference on New Developments in Soil Mechanics and Geotechnical Engineering, Near East University, Nicosia, TRNC (2022)
10. V. Fioravante, D. Giretti. *Acta Geotech* **11**, 953-968 (2016)
11. ASTM D698-12(2021), Standard Test Methods for Laboratory Compaction Characteristics of Soil Using Standard Effort (12,400 ft-lbf/ft<sup>3</sup> (600 kN-m/m<sup>3</sup>)), ASTM International, West Conshohocken, PA, 2021, [www.astm.org](http://www.astm.org).
12. O. Wendroth, W. Ehlers, J. Hopmans, H. Kage, J. Halbertsma, J. Wosten. *Soil Science Soc of America J* **57**, 1436-1443 (1993)
13. M. Nicotera, R. Papa, G. Určiuoli. *Geot Test J* **33**, 263-285 (2010)
14. M.R. Taha, M.H. Kabir. *Env Geology* **47**, 375-381 (2005)
15. E. Birle, D. Heyer, N. Vogt. *Acta Geo* **3**, 191-200 (2008)
16. T.W. Lambe. Spec Tech Publ No. 163, Am Soc Test Mater (ASTM), Philadelphia, 56-67 (1954)
17. E.C. Lawton, R.J. Frigaszy, M.D. Hetherington. *J Geotech Eng* **118**, 1376-1394 (1992)
18. V. Ferber, J.C. Auriol, Y.J. Cui, J.P. Magnan. *Can Geotech J* **45**, 252-265 (2008)
19. S.M. Rao, K. Revanasiddappa. *J Geotech Geoenviron Eng* **126**, No. 1, 85-90 (2000)
20. A.S. Dias, A. Kamath, M. Pirone, G. Určiuoli. *E3S Web of Conferences* **195**, 03003 (2020)
21. A.S. Dias, M. Pirone, M.V. Nicotera, G. Určiuoli. *Geomech Energy Environ* **30**, 100235 (2022a)
22. A.S. Dias, M. Pirone, M.V. Nicotera, G. Určiuoli. *Acta Geotech* **17**, 837-855 (2022b)
23. M.T. Van Genuchten. *Soil Science Soc of America J* **44**, 892-898 (1980)
24. X. Hou, S. Qi, T. Li, S. Guo, Y. Wang, Y. Li, L. Zhang. *Eng Geology* **277**, (2020)
25. P. Delage, M. Audiguier, Y.J. Cui, M. Howat. *Can Geot J* **33**, 150-158 (1996)
26. D.G. Fredlund, A. Xing, S. Huang. *Can Geot J* **31**, 533-546 (1994)
27. C.W.W. Ng, Y.W. Pang. *J Geot Geoenviron Eng* **126**, 167-188 (2000)